EPJ Web of Conferences **302**, 16005 (2024) https://doi.org/10.1051/epjconf/202430216005
SNA + MC 2024

Simulation of the DD, TT and DT JET Neutron Streaming Experiments with TRIPOLI-4® Monte-Carlo code

Jean-Baptiste Pontier[1,*], *Johan* Cufe[1,†], *Thibault* Moulignier[1,‡], and *JET Contributors*[§]

[1]Université Paris-Saclay, CEA, Service d'étude des réacteurs et de mathématiques appliquées, 91191 Gif-sur-Yvette, France

Abstract. The DD, TT and DT neutron streaming experiments (NEXP-STRE) in the fusion facility JET are here simulated with TRIPOLI-4® Monte-Carlo code. Specifically, we present the results from the simulation of the DD (2019) and the later TT and DT (2021) campaigns. The last version of TRIPOLI-4® code, developed by CEA, is provided with an innovative variance reduction technique based on the adaptive multi-level splitting (AMS) methodology for particle transport which ensures reliable results in very detailed, complex and vast geometry. Furthermore, a specific tool, developed by CEA, is used to automatically convert MCNP geometry into TRIPOLI-4® geometry format, which allows to perform fast and reliable comparisons between the results obtained by the mean of both calculation tools. The JET 360° MCNP model is used as a basis for creating the TRIPOLI-4® geometry. The neutron flux and doses in thermoluminescent detectors (TLDs) and reaction rates in activation foil (AF) detectors are computed for various positions in the experimental hall. A comparison of our results with the experimental values (2019 DD - 2021 TT campaigns) and the MCNP computed values (all campaigns) is presented. The AMS results crucial for obtaining statistically reliable quantities with TRIPOLI-4® code.

1 Introduction

The Joint European Torus (JET) is a fusion tokamak located on the UKAEA campus in Culham, UK. It is used as a research experiment for various nuclear fusion topics, in particular in support of the ITER (International Thermonuclear Experimental Reactor) program. The knowledge of neutron flux and doses around the ITER experiment when it is running and after a shutdown are mandatory for the nuclear operator, allowing safe maintenance operation in the nuclear installation. These data are often computed with Monte-Carlo (MC) codes like TRIPOLI-4® in the case of a fission reactor, but the technological and physical specificities of fusion reactor oblige us to supplement the validation basis of the simulation tools with experimental and numerical validation on the fusion experiment. For this purpose, three experimental campaigns of neutron streaming experiments performed at JET since 2016, within the WPPrIO work package of the EUROFUSION organisation, have been reproduced by various Monte Carlo codes, including TRIPOLI-4® code. This work is about the analysis of the

* e-mail: jean-baptiste.PONTIER@cea.fr † e-mail: johan.CUFE@cea.fr ‡ e-mail: thibault.MOULIGNIER@cea.fr § See the author list of "Overview of T and D-T results in JET with ITER-like wall" by CF Maggi et al., Nuclear Fusion Special Issue: Overview and Summary Papers from the 29th Fusion Energy Conference (London, UK, 16-21 October 2023)

simulated Deuterium-Deuterium (DD) campaign led in 2019 and the Tritium-Tritium (TT) and Deuterium-Tritium (DT) campaigns which took place in 2021. During these experimental campaigns, two types of specifically designed detectors have been installed at various positions in the JET Hall to measure the neutron flux during the tokamak operations. The first type of detector uses the thermoluminescent detector (TLD) technology and the second type uses the neutron activation foil technology (AF) to assess the neutron fluence (flux integrated over the operation time). Among the 23 detector positions chosen for measuring the neutron flux and doses, some are close to the machine and are irradiated with a strong neutron flux and others are located up to 40 meters from the source behind very high attenuation materials. In the first case, the computation of neutron transport and estimation of the flux are quite classical for Monte-Carlo code whereas in the second case, the estimation of neutron-related quantities is very challenging for the code (high attenuation and tiny solid angle covered by the TLD and AF volumes). For instance, to ensure radiation protection for workers in the JET installation after nuclear operations, the southwest labyrinth and the southeast chimney have to be closely studied, as there are paths where the radiation shielding (concrete walls) is discontinued. To ensure reliable comparison with MCNP results and efficient development of the input data for TRIPOLI-4® code, the geometry and the compositions of the materials used in the simulation are automatically converted [1] from the MCNP input data provided by UKAEA in the framework of WPPrIO organisation. The geometry of the tokamak and the tokamak hall are shown in Fig. 1.

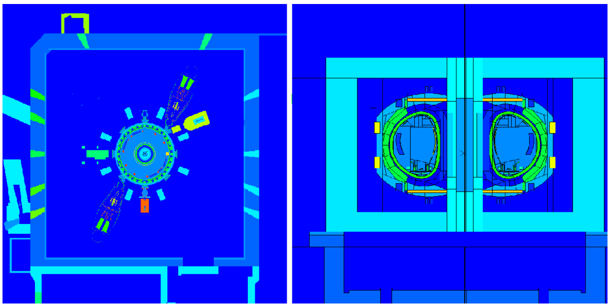

Figure 1. Radial (left) and axial (right) view of the JET 360° geometry.

The AMS (Adaptive Multilevel Splitting) variance reduction technique is used to achieve a low statistical uncertainty on the results, especially at the most distant detector locations. The general Monte-Carlo approach and the innovative variance reduction method of AMS in TRIPOLI-4® are presented in Section 2. The description of the streaming experiments follows in Section 3. Then, Section 4 covers the results obtained for the analysis of DD, TT and DT campaigns. Finally, the article ends with the conclusion in Section 5.

2 Neutral particle transport methodology

The transport of neutral particles like neutrons and photons is described by the well-known integro-differential Boltzmann equation. The widely used approach to simulate the transport of this kind of particles in a fusion facility, like the Joint European Torus (JET), is the MC approximation. The solution of the transport equation by the latter methodology is based on the simulation of a very large number of random trajectories inside the domain. The trajectory of each particle is simulated individually, from emission to absorption, and its interaction with matter is modelled in agreement with the underlying physical laws. The averages over all the simulated trajectories allow the estimation of physical quantities of interest, for instance, reaction rates, neutron fluence and dose rates [2]. The MC method is a statistical method, hence results are always needed with associated confidence intervals, which decrease with a square-root dependency on the number of simulated particles. For the reason mentioned above, MC calculations usually require large amounts of computer processing time but doubtless advantages are offered, among all the ability to deal with arbitrarily complex geometries, as it is the case of large fusion facilities, without introducing any discretization approximation. However, with simulations of rare events such as radiation protection problems, usually fewer simulated histories will contribute to the requested response. This usually leads to large statistical errors on the computed average quantities. To increase the probability of sampling rare events of interest and hence reduce the statistical error, variance reduction techniques (VRTs) are introduced.

2.1 TRIPOLI-4® general code overview

The MC particle transport code TRIPOLI-4® is developed by CEA. This MC code is capable of simulating neutral particles among which neutrons, photons and charged ones like positrons and electrons in three-dimensional geometries, with a continuous energy treatment. TRIPOLI-4® has been extensively devoted to reactor physics, criticality safety, radiation shielding and nuclear instrumentation applications in both fission and fusion systems. However, this is the first time that simulations of Streaming Experiments in large fusion facilities are performed. Regarding the code structure, it heavily relies on object-oriented programming and makes use of class definitions to simulate the physics of the system under study. For the sake of brevity, we summarize those in three classes: the particle, geometry-composition and response class, which are common classes although syntactically different from other MC codes available in the scientific community (e.g. MCNP, OpenMC) [9, 10]. An automatic tool that converts geometry from the MCNP input format into the TRIPOLI-4® format has been employed for our simulations. Most of the idiomatic MCNP constructs, such as universes, lattices, macro-bodies and affine coordinate transformations are handled [1]. TRIPOLI-4® is also equipped with various VRTs, whose general idea is to replace the natural laws of flight and collisions with some "artificial" laws to increase the probability of sampling rare events. Here, we focus our attention on the recently developed AMS algorithm for transport applications, which has been used in our calculations. For a more in-depth description of TRIPOLI-4® architecture and features the reader is referred to [3].

2.2 AMS overview in TRIPOLI-4®

The original AMS algorithm was first proposed by Cerou and Guyader in the field of Applied Mathematics [4]. The main purpose was to help the computation of rare events in the case of Markov chains. The methodology has been recently adapted to the field of particle transport by Louvin et al. for attenuation and shielding problems in non-multiplying media [5].

As mentioned, the AMS algorithm is applicable whether an association to a Markov chain is possible. The definition of a function which quantifies the importance of the Markov chain itself is also necessary for the algorithm. In the case of a MC particle simulation, each particle trajectory is built as a step-by-step process, meaning that the state of a particle at a given time is determined exclusively from the knowledge of its state after the previous interaction. Hence, the sequence of the phase space of the particle at the successive interaction can be considered a discrete-time Markovian process [5]. Indeed, this sequence is identified with the particle's *track*.

The idea behind the AMS algorithm is to push the initially simulated particles towards the region of interest. The AMS in TRIPOLI-4® is implemented as an iterative algorithm, initialized with an analog simulation, and consists of three major steps: sorting, splitting and scoring. During the first iteration, N particles are tracked until their death[1]. These N different tracks are followed during the next iterations. The first AMS step consists of the definition of an importance function which is associated with the geometry. This is necessary to determine which regions are of major interest to the simulation. The importance is related to the probability, for a particle located in a generic point P, to contribute to the requested response. Let us define this importance function as $I(P) = I(\vec{x}, \vec{\omega}, E)$, with $\vec{x}, \vec{\omega}$ and E being the position, direction and energy of the particle, respectively. This importance function is said to be "relative" since it only ranks particles with respect to each other, with the value of the importance on its own being meaningless. We introduce $S = [P_0, \ldots, P_M], M \in \mathbb{N}$ and $I(S) = \max I(P_i), i \in [0, M]$ which are the the particle track, with P_i representing the properties of the particle surviving its i-th collision in the medium (total of M collisions) and the importance of a particle track, respectively. At the end of an iteration, tracks are ranked according to their importance $I(S_j)$, $j \in [1, N]$, with the ranking defined by the maximum importance reached during the simulation by the branches inside that track. In TRIPOLI-4®, the only constrained to the importance function, no matter its definition[2], is that it is higher than an arbitrarily defined constant. However, this is always ensured since any point in the area of interest is given a numerical infinite importance (maximum float point).

Then, a splitting step is defined as the k-th smallest value in the sample $[I(S_1), \ldots, I(S_N)]$, and all the k_j tracks having an importance lower or equal to that level are discarded. The next step consists of the resampling of the k_j deleted tracks. For each of them, one of $N - k_j$ surviving ones is randomly selected and split at its first point whose importance is higher than the splitting level. In this way, the system contains the same number of original N tracks. New iterations are started and the whole process is repeated until at least $N - k_j + 1$ tracks have reached the region of interest [7]. As the last step, an unbiased estimator for any generic score ϕ in the region of interest can be constructed as

$$\hat{\phi}_{AMS} = w_j \phi, \quad w_j = \prod_{z=1}^{j} \left(1 - \frac{k_z}{N}\right), \tag{1}$$

with w_j a cumulated weight factor (equal for all the particles) to keep the result unbiased and k_z the number of re-sampled tracks at iteration z. From the user point of view in TRIPOLI-4®, the AMS simulation needs mainly the specification of the type of importance function. For instance, the AMS can be equipped with an importance map coming from the INIPOND module or the CADIS method [6]. Among the other importance functions, the purely spatial importance with decreasing or increasing importance with the distance to the spatial object is also available. Indeed, the point-object spatial importance function is adopted in our simulations. The AMS has been generally proven to be a valid alternative to existing VRTs in complex configurations [5].

3 Description of the streaming experiments

The experimental setup during the NEXP-STRE campaign was composed of 23 detectors (identified by their position numbered A1 to A8, B1 to B8 and C1 to C7), all of them containing thermoluminescent detectors and 5 of them contained activation foils. The detector positions in the JET hall are represented in Fig. 2 (C3 has been moved to position C7 for TT and DT experiments).

[1] Absorbed or leaked out of the geometry. [2] The selection of the importance function is crucial for the AMS algorithm efficiency, as proven in [4].

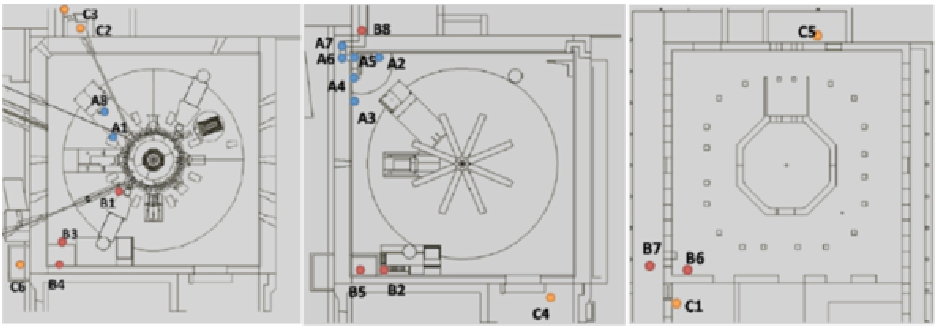

Figure 2. Positions of TLDs and AFs for the DD (2019) experiment.
From left to right: midplane, ground floor and basement (x-y plane) [13].

The detectors are placed both closely and far from the neutron source. One of the main interests of these calculations is to prove the capability of the Monte-Carlo codes to assess the efficiency of the biological shield and the penetrations in the concrete wall. This is the reason why most of the detectors are placed close to the southwest labyrinth (A series) and southeast chimney (B series). These two discontinuities are respectively used as an entry in the torus hall composed of borated concrete and a path from the basement floor to the torus hall. The size of the entire simulated geometry is up to 50 x 50 x 35 m (x, y, z), in which the JET hall plus the biological shielding (concrete wall) occupies a 40 x 40 x 35 m. The detector is composed of a surrounding HDPE cylinder that acts as a container for detecting TLD pellets and activation foils, the cylinder is 25 cm high and 25.5 cm in diameter. There are 20 TLDs in each detector, divided into two groups of 10, the first is held in a rectangular polyethylene holder and the second in a circular holder. Each of the pellets is 0.9 mm thick and 4.5 mm diameter. The rectangular holder is facing the tokamak in a vertical position whereas the circular holder is facing the z plane in a horizontal position inside the container. This geometric arrangement has been set to study the directionality of the neutron flux which however is not investigated in our simulations. Each of the AFs consists of high-purity cobalt, silver and tantalum disc-shaped foils (15 mm diameter, 0.50 mm thick), placed at the centre of the polyethylene holders (same as TLDs), and used to assess the reaction rates during the 2021 TT campaign. The design and TRIPOLI-4® representation of the TLDs and AFs are given in Figure 3. To be able to discriminate the dose induced by neutrons in the detector from

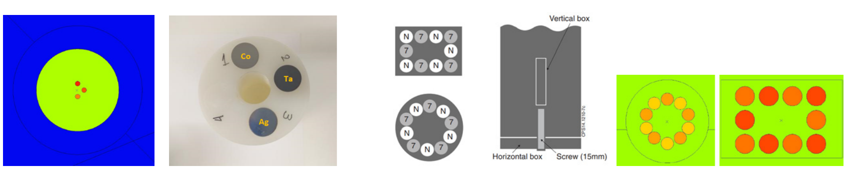

Figure 3. TRIPOLI-4® representation (x-y plane) and experimental set [12] of the AFs (left) and TLDs (right) inside the holders.

the dose induced by other particles such as gammas, two types of TLDs were used, respectively named MCP-N and MCP-7. The main difference between the two types is the isotopic composition of Lithium used, MCP-N type is composed of natural lithium containing 7.59% of ^{6}Li and MCP-7 type is composed of ^{7}Li enriched lithium (99.97%). The neutron capture cross section of MCP-N TLDs is then far higher than the neutron capture cross section of MCP-7, this very low concentration in ^{6}Li makes this last practically insensitive to neutrons.

4 Results

4.1 TRIPOLI-4® JET calculations and model description

The 360° JET model for TRIPOLI-4® was created with the conversion of the MCNP model developed by the Culham Center for Fusion Energy by means of a dedicated tool developed by CEA [1]. The resulting geometry contains about 12,500 volumes. The composition of materials and the association between the geometry and the materials are also supported by the converter, thus allowing a very high level of confidence in the comparison between results provided by both codes. For each of the three sources used, the spatial distribution of the neutron source remains the same. A visualization of the source distribution is shown in Figure 4. The energy spectrum of the source is integrated into TRIPOLI-4® for DD and DT fusion reactions and it has been converted from the MCNP input for the TT reaction. The transport phenomenon has been simulated with TRIPOLI-4® code in his 11.0 (DD) and 12.0 (TT and DT) versions using the JEFF-3.2 and ENDF/B-VII.1 nuclear data libraries [14].

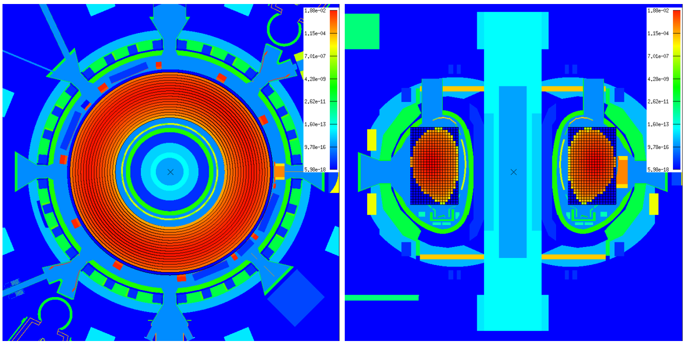

Figure 4. Toroidal and poloidal distributions of the JET neutron source used in TRIPOLI-4® calculations.

4.2 Neutron flux map in the JET torus hall

The neutron flux map over the whole geometry (Figure 5) has been computed using an extended mesh in TRIPOLI-4®. The mesh is centred on the origin of the model and each cell is 25 x 25 x 500 cm. This calculation took 18,500 CPU hours and no variance reduction technique was used. The deep blue colour represents the zone where no flux has been tallied. Regarding the cells inside the torus hall, the 1σ statistical uncertainty on the flux is below 10%, this value may rise to 50% in the concrete wall shielding. This result illustrates the mandatory use of advanced reduction techniques such as AMS to assess the flux in TLDs and AF detectors around the tokamak. The main drawback of using an importance which changes with the detector's position is the need to run one calculation per detector.

4.3 NEXP-STRE TLDs simulation

The results of neutron fluence computed on the TLDs are here presented for the TRIPOLI-4® simulation. As of today, experimental results on neutron fluence measurement with TLDs are

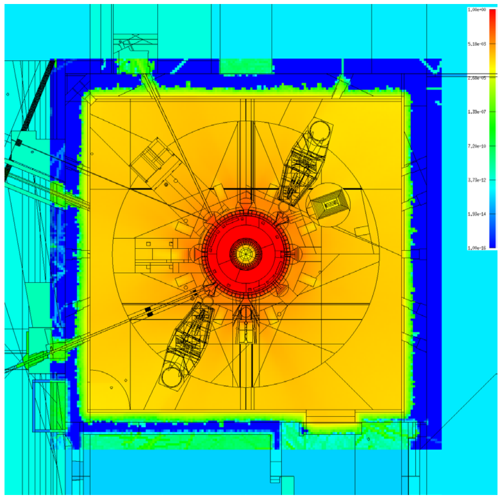

Figure 5. Radial neutron Flux map centred on the Z = 0 cm plane.

available only for the 2019 DD campaign [13], these results are also compared to MCNP simulations [15]. To ensure a rigorous comparison, all the results are given per JET neutron source.

4.3.1 Neutron fluence in TLDs

As previously stated, one calculation per detector position and neutron source has been made to compute the neutron flux in TLDs. In each of these calculations, the AMS variance reduction technique targeted the 20 TLD pellets of the studied detector. The final result is averaged over the 20 TLD pellets (10 in circular holder and 10 in rectangular holder) of the studied detector. Given that the fluence result is a linear combination of each of the values obtained on individual pellets, equally weighted, the final MC error on the result is given by $MC\sigma_{final} = \frac{1}{\sqrt{n}}\sqrt{\sum_{i=1}^{n} MC\sigma_i^2}$. The top of Figure 6 shows the simulation results obtained for the three studied neutron source energy spectra (DD, TT and DT) and the 2019 DD experimental values. For each series, the positions are ranked from left to right in function of their distance to the neutron source. B7 and B8 position results are not shown because the experimental values are below the background level (10^{-14} n cm^{-2}). The bottom of the figure shows the computed over experimental (C/E) results for the 2019 DD campaign for both TRIPOLI-4® and MCNP [13]. The uncertainty on C/E and C/C ratio are computed from the uncertainty on each value using the following: $\sigma^2(C/E) = \left(\frac{C}{E}\right)^2\left(\frac{\sigma_C^2}{C^2} + \frac{\sigma_E^2}{E^2}\right)$. At all the positions studied in this work, the flux computed for different source energy spectra is very close, a slight increase of the flux is observed with the DT source, mainly due to the higher average energy of the neutron emitted in this reaction. A clear trend of an increase in the C/E value, when the distance to the source grows, is observed for both codes. This overestimation of the flux by the code can be explained by the impact of geometric approximations (lack of absorbing material because of non-represented devices such as large equipment or heating systems around the tokamak) or uncertainty on the material compositions that may be more and more significant when the flux decreases. The uncertainty on the boron concentration in the concrete of the wall may have a significant impact on the C/E results, especially at the detector positions located near the wall or in the complex concrete environment (maze or chimney). The C/E computed with TRIPOLI-4® results ranges from 0.8 to about 8 for the most distant positions studied, these values are of the same order of magnitude as those observed by other teams working on this computational model of JET [13, 15]. Table 1 presents the C/C results (indicated as R_C) obtained with TRIPOLI-4® and MCNP for the three different neutron sources at various locations. The C/C uncertainty is given here in absolute value.

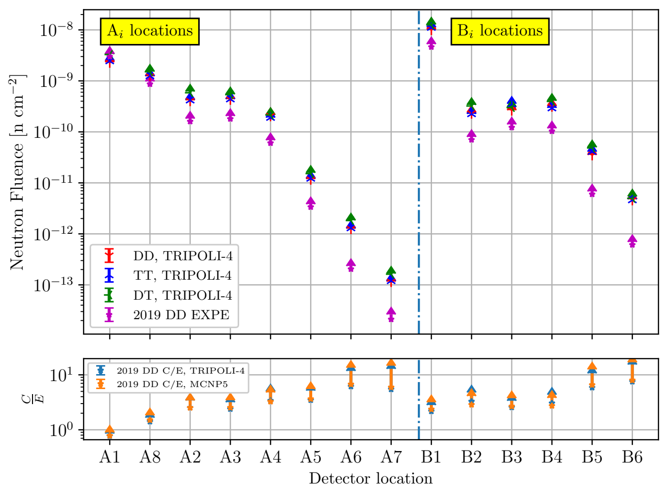

Figure 6. Computed fluence per neutron source at various positions for DD, TT and DT neutron source spectrum (top) - C/E ratios on the 2019 DD campaign (bottom). Positive 1σ showed only.

Table 1. R_C ratio between TRIPOLI-4® and MCNP5 and absolute statistical quantities.

Positions	DD		TT		DT	
	R_C (1σ)	$\lvert(1 - R_C)/1\sigma\rvert$	R_C (1σ)	$\lvert(1 - R_C)/1\sigma\rvert$	R_C (1σ)	$\lvert(1 - R_C)/1\sigma\rvert$
A1	0.97 (0.10)	0.27	0.99 (0.15)	0.05	0.99 (0.02)	0.40
A8	0 94 (0.09)	0.65	0.98 (0.02)	1.21	0.97 (0.02)	1.31
A2	1.01 (0.10)	0.05	1.02 (0.04)	0.37	1.01 (0.08)	0.15
A3	0.96 (0.10)	0.46	1.01 (0.04)	0.40	0.95 (0.02)	1.84
A4	1.04 (0.11)	0.34	0.98 (0.01)	1.57	1.00 (0.02)	0.27
A5	0.96 (0.10)	0.45	0.98 (0.03)	0.76	0.96 (0.04)	1.21
A6	0.91 (0.10)	0.85	0.99 (0.01)	2.17	1.02 (0.01)	2.32
A7	0.92 (0.09)	0.87	1.00 (0.01)	0.66	1.02 (0.03)	0.72
B1	0.92 (0.09)	0.86	0.99 (0.03)	0.43	0.95 (0.04)	1.11
B2	1.15 (0.23)	0.63	0.98 (0.02)	1.28	1.10 (0.07)	1.46
B3	0.81 (0.08)	2.29	1.05 (0.04)	1.25	1.00 (0.03)	0.08
B4	1.12 (0.11)	1.05	0.99 (0.03)	0.37	1.08 (0.04)	1.86
B5	0.89 (0.09)	1.19	1.02 (0.01)	1.52	1.01 (0.03)	0.46
B6	0.94 (0.13)	0.43	0.92 (0.05)	1.52	0.75 (0.09)	2.92
B7	1.02 (0.11)	0.22	1.02 (0.03)	0.56	0.95 (0.06)	0.79

For the vast majority of the positions studied, the results are statistically compatible to 1σ and almost all of them are compatible to 2σ. The residual source of discrepancies between the two calculations is the use of different nuclear data libraries. The C/C ratio might be lowered in future simulations with the use of the FENDL library.

4.4 NEXP-STRE AFs simulation

In this section, the results of the NEXP-STRE AFs experiments in the TT campaign are presented. Although referred to a single campaign, different neutron sources are simulated [13]. Some residuals of deuterium in the chamber were detected during the TT campaign and the proportions of the contributions to the neutron source were accordingly set to 40% and 60% for the DT and TT sources, respectively. DD contributions were neglected since the contribution to the neutron source was less than 0.5%. Reaction rates (RRs) using dosimetry nuclear data files (IRDFF-II / IRDF-2002) were computed using MCNP5 and TRIPOLI-4®. Specifically, the radiative capture was the requested reaction. No difference for the radiative capture cross section is present for the two libraries [16]. The relative results for each of the neutron sources (DT-TT) are presented in Table 2 and Table 3.

Table 2. Computed RRs$^{n,\gamma}$ (s^{-1}) for the NEXP-STRE foils with DT neutron source. †MCNP5 ($\sigma^{IRDFF-II}$), ‡TRIPOLI-4® ($\sigma^{IRDF-2002}$), *TRIPOLI-4® ($\sigma^{ENDF/B-VII.1}$)

Isotope	A1	A2	A4	B2	B3
Co60†	4.98E-10(2%)	9.99E-11(4%)	4.88E-11(3%)	6.56E-11(3%)	9.28E-11(5%)
Co60‡	4.04E-10(2%)	7.98E-11(5%)	4.07E-11(3%)	5.90E-11(4%)	8.64E-11(3%)
Co60*	9.47E-11(3%)	5.84E-11(5%)	4.03E-11(3%)	5.51E-11(4%)	8.07E-11(4%)
Ta182†	2.06E-10(2%)	4.24E-11(3%)	2.16E-11(3%)	2.32E-11(2%)	3.26E-11(3%)
Ta182‡	1.67E-10(2%)	3.47E-11(5%)	1.92E-11(4%)	2.80E-11(4%)	1.42E-11(4%)
Ta182*	3.93E-11(3%)	2.25E-11(3%)	1.90E-11(4%)	2.00E-11(4%)	3.10E-11(6%)
Ag110^m†	**2.26E-11(2%)**	**4.13E-12(4%)**	**2.07E-12(4%)**	**1.90E-12(2%)**	**2.54E-12(3%)**
Ag110^m‡	**1.94E-11(2%)**	**3.41E-12(4%)**	**1.70E-12(4%)**	**1.73E-12(4%)**	**2.13E-12(3%)**
Ag110^m*	**9.63E-11(2%)**	**4.50E-11(4%)**	**3.73E-11(4%)**	**3.33E-11(5%)**	**4.50E-11(4%)**

In addition, Table 4 shows the results for both DT-TT neutron sources simulated in the same calculation with the proportions mentioned above. Noticeably, the use of transport cross section libraries, specifically the ENDF/B-VII.1 does not lead to noticeable changes in the results, with the only exception of the Ag110^m (values in bold). This behaviour should be investigated more for other metastable isotopes. Indeed, dosimetric cross sections are

Table 3. Computed RRs$^{n,\gamma}$ (s^{-1}) for the NEXP-STRE foils with TT neutron source. †MCNP5 ($\sigma^{IRDFF-II}$), ‡TRIPOLI-4® ($\sigma^{IRDF-2002}$), *TRIPOLI-4® ($\sigma^{ENDF/B-VII.1}$)

Isotope	A1	A2	A4	B2	B3
Co60†	3.94E-10(1%)	7.91E-11(1%)	3.86E-11(1%)	5.89E-11(1%)	8.11E-11(1%)
Co60‡	5.17E-10(3%)	9.80E-11(4%)	4.88E-11(3%)	.75E-11(3%)	9.57E-11(4%)
Co60*	1.22E-10(4%)	6.78E-11(5%)	5.98E-11(3%)	7.49E-11(4%)	9.13E-11(4%)
Ta182†	1.63E-10(1%)	3.38E-11(1%)	1.74E-11(2%)	2.05E-11(1%)	2.89E-11(1%)
Ta182‡	2.09E-10(3%)	3.96E-11(4%)	2.14E-11(2%)	2.50E-11(4%)	2.87E-11(3%)
Ta182*	5.07E-11(3%)	2.91E-11(5%)	2.71E-11(4%)	2.51E-11(4%)	3.29E-11(4%)
Ag110^m†	**1.89E-11(1%)**	**3.30E-12(1%)**	**1.69E-12(2%)**	**1.65E-12(1%)**	**2.17E-12(1%)**
Ag110^m‡	**2.27E-11(3%)**	**3.59E-12(4%)**	**1.99E-12(4%)**	**1.93E-12(3%)**	**2.72E-12(5%)**
Ag110^m*	**1.16E-10(3%)**	**5.84E-11(6%)**	**5.37E-11(5%)**	**4.18E-11(6%)**	**5.60E-11(6%)**

always suggested for these types of reaction rate calculations. Both MCNP and TRIPOLI-4® codes provide scores within a maximum uncertainty of $1\sigma \leq 6\%$. Indeed, a good agreement between the two codes is found for all the detector positions.

Table 4. Computed $RRs^{n,\gamma}$ (s^{-1}) for the NEXP-STRE foils in TT 60% - DT 40% campaign. †MCNP5 ($\sigma^{IRDFF-II}$), ‡TRIPOLI-4® ($\sigma^{IRDF-2002}$)

Isotope	A1	A2	A4	B2	B3
Co60†	4.36E-10(1%)	8.74E-11(2%)	4.27E-11(1%)	6.15E-11(1%)	8.58E-11(2%)
Co60‡	4.72E-10(2%)	9.07E-11(3%)	4.55E-11(2%)	8.21E-11(3%)	9.20E-11(3%)
Ta182†	1.80E-10(1%)	3.73E-11(1%)	1.91E-11(2%)	2.16E-11(1%)	3.04E-11(1%)
Ta182‡	1.92E-10(2%)	3.76E-11(3%)	2.05E-11(2%)	2.62E-11(3%)	1.78E-11(3%)
$Ag110^m$†	2.04E-11(1%)	3.63E-12(2%)	1.84E-12(2%)	1.75E-12(1%)	2.32E-12(1%)
$Ag110^m$‡	2.14E-11(2%)	3.52E-12(3%)	1.87E-12(3%)	1.85E-12(3%)	2.48E-12(3%)

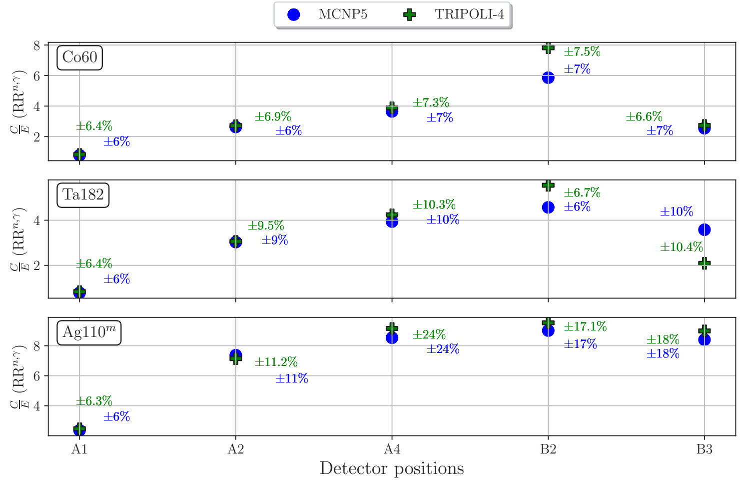

Figure 7. C/E ratio of $RRs^{n,\gamma}$ (1σ in per cent) using MCNP5 and TRIPOLI-4®.

The comparison with the experimentally determined values through the Computed/Experimental (C/E) ratio is also shown in Figure 7. The ratio varies from a minimum of 0.7 to a maximum of 9.5. The reported uncertainties have been calculated including all identified sources of error, namely the statistical uncertainty on the RRs in the simulation and the uncertainties on the experimental values. The associated experimental uncertainties are relevant due to the detector's efficiency and the correction factors uncertainties, leading to higher uncertainties due to error propagation. Detectors at positions B2 and B3, located in the South East (SE) chimney area, were characterized in general by the highest C/E values and most relevant uncertainties.

5 Conclusion

The work presented in this paper was dedicated to reproducing with the CEA Monte-Carlo code TRIPOLI-4® the neutron streaming experiments performed at JET tokamak during three experimental campaigns, the 2019 DD campaign and the 2021 TT and DT campaigns. Two types of experiments have been simulated. The first type is neutron flux measurement around the machine and toward JET installation shielding penetrations with thermoluminescent detectors and the second type is neutron-induced reaction rate measured with activation foils detectors. The geometry and compositions were successfully obtained by the conversion of the MCNP input by the mean of a specific tool developed for TRIPOLI-4®. An advanced and innovative variance reduction technique based on neutron population control called AMS was used to assess the flux and reaction rates in tiny volumes of detection and behind attenuation factor up to 10^{13} with low statistical uncertainty. The comparison of the results obtained with TRIPOLI-4® has been done both with other numerically obtained results and with experimental values when available. Regarding the TLD experiment, C/E values range from 0.8 to 8, increasing when the distance to the source increases, these results might be explained by the geometrical approximations and various uncertainties in the experimental conditions. Similar magnitudes were also found for the C/E ratio on the reaction rates in AFs. MCNP5 and TRIPOLI-4® codes converge to results of the same magnitude and with confidence intervals of a few per cent only. The study on the NEXP-STRE on AFs is also propaedeutic for the NEXP-SDR (shut-down dose rate) experiment, which will be simulated by TRIPOLI-4® in future research. The C/C values are close to unity at almost all the positions of the detector studied and always statistically compatible (difference below 3σ). Further simulations could be performed again with the FENDL library to improve the C/C ratio and to perform a sensitivity analysis on boron concentration in concrete to improve the C/E ratio far from the source. This work contributes to the demonstration of TRIPOLI-4® code's ability to simulate very complex and challenging geometry and large systems like a tokamak and its close environment.

Acknowledgment

TRIPOLI-4® is a registered trademark of CEA. The authors gratefully acknowledge EDF and Framatome for their long-term partnership and their support.

The authors are specifically grateful to Yannick Peneliau (CEA-Cadarache) for the numerous discussions about the simulations performed in this study. Special thanks to Steve Bradnam and Luke Jones (UKAEA), Igor Lengar from (JSI), Theodora Vasilopoulou (NCSRD), Mariusz Kłosowski (IFJ), and Rosaria Villari (ENEA) for the technical and physical contributions on the NEXP-STRE project.

This work has been carried out within the framework of the EUROfusion Consortium, funded by the European Union via the Euratom Research and Training Programme (Grant Agreement No 101052200 — EUROfusion). Views and opinions expressed are however those of the author(s) only and do not necessarily reflect those of the European Union or the European Commission. Neither the European Union nor the European Commission can be held responsible for them.

References

[1] D. Mancusi, *Automatic conversion of MCNP geometries to TRIPOLI-4®*, Proceedings of the international conference on physics of reactors-PHYSOR 2022.

[2] Lux, I. and Koblinger L., *Monte Carlo Particle Transport Methods: Neutron and Photon Calculations*, CRC Press, 1991.

[3] E. Brun, F. Damian, C.M. Diop, E. Dumonteil, F.X. Hugot, C. Jouanne, Y.K. Lee, F. Malvagi, A. Mazzolo, O. Petit, J.C. Trama, T. Visonneau, A. Zoia, *TRIPOLI-4®, CEA, EDF and AREVA reference Monte Carlo code*, Annals of Nuclear Energy 82, 151-160 (2015).

[4] F. Cérou, A. Guyader, *Adaptive multilevel splitting for rare event analysis*, Stochastic Analysis and Applications, Taylor & Francis, 2007.

[5] Louvin, Henri and Dumonteil, Eric and Lelièvre, Tony and Rousset, Mathias and Diop, Cheikh M. *Adaptive multilevel splitting for Monte Carlo particle transport*, EPJ Web of Conferences, Volume 153, 6006, 2017.

[6] D. Mancusi, M. Nowak, E. Dumonteil, H. Louvin, E. Masiello, and D. Sciannandrone. *Evaluating importance maps for TRIPOLI-4® using deterministic or on-line methods*, RPSD 2018-20th Radiation protection and shielding division: Topical Meeting, 2018.

[7] K. Fröhlicher, E. Dumonteil, L.Thulliez, J. Taforeau, M. Brovchenko. *Improving the variance in Monte Carlo criticality calculations with adaptative multilevel splitting*, PHYSOR2022 - International Conference on the Physics of Reactors, American Nuclear Society (ANS), May 2022, Pittsburgh, United States, irsn-03948886.

[8] B. Obryk, R. Villari, P. Batistoni, A. Colangeli, P. De Felice, N. Fonnesu, M. Ktosowski, S. Loreti, K. Malik, J. Nash, M. Pillon, M. Pimpinella, L. Quintieri and JET Contributors, *TLD calibration for neutron fluence measurements at JET fusion facility*, Nuclear Inst. and Methods in Physics Research, 202-213, 2018.

[9] B. Forrest and Barrett, RF and Booth, TE and Bull, JS and Cox, LJ and Forster, RA and Goorley, TJ and Mosteller, RD and Post, SE and Prael, RE and others, *MCNP version 5*, Trans. Am. Nucl. Soc, pag 02–3935, 2002.

[10] R. Paul K and Horelik, N. and Herman, B. and Nelson, A. and Forget, B. and Smith, K. *OpenMC: A state-of-the-art Monte Carlo code for research and development*, Annals of Nuclear Energy, 82, 90–97, 2015, Elsevier.

[11] T. Vasilopoulou, I. E. Stamatelatos, P. Batistoni, A. Colangeli, D. Flammini, N. Fonnesu, S. Loreti and JET Contributors, *Improved Neutron Activation Dosimetry for Fusion*, Fusion Engineering and Design 139: 109-114, 2019.

[12] P. Batistoni et al. *Benchmark experiments on neutron streaming through JET Torus Hall penetrations*, Nuclear Fusion 55 (2015).

[13] Bor Kos, Georgette Radulescu, Robert Grove, Rosaria Villari, Paola Batistoni & JET Contributors (2023). *Comprehensive Analysis of Streaming and Shutdown Dose Rate Experiments at JET with ORNL Fusion Neutronics Workflows*, Fusion Science and Technology.

[14] OECD/NEA, *The JEFF-3.2 Nuclear Data Library*, NEA Data Bank, Available at https://www.oecd-nea.org/dbforms/data/eva/evatapes/je 32/, 2014.

[15] Jonathan David Naish, P. Batistoni, B. Kos, B. Obryk, R. Villari, T. Vasilopoulou, I.E. Stamatelatos, *Comparison of neutron flux streaming calculations to the 2019-2020 JET Experimental Deuterium-Deuterium Results*, Fusion Engineering and Design, Volume 170, 2021, 112538, ISSN 0920-3796.

[16] Soppera, Nicolas and Bossant, Manuel and Cabellos, Oscar and Dupont, Emmeric and Díez, Carlos J, *JANIS: NEA Java-based nuclear data information system*, EPJ Web of Conferences, 2017, EDP Sciences.